# Appendix: Detailed Wind Farm Model and IEEE 14-bus System

Zilong Gong, Junyu Mao, Adrià Junyent-Ferré, *Senior Member, IEEE*, and Giordano Scarciotti, *Senior Member, IEEE*

## NOMENCLATURE

**Roman symbols**

| | |
|---|---|
| $A$ | Wind turbine swept surface |
| $C$ | DC bus capacity |
| $I_t$ | One-mass wind turbine aggregated inertia |
| $K_{C_p}$ | Constant tip speed ratio speed control law coefficient |
| $L_l$ | Inductance of the grid connection impedance |
| $P$ | Generator pole pairs |
| $Q_s$ | Generator stator reactive power |
| $R$ | Wind turbine radius |
| $V_{DC}$ | DC bus voltage |
| $V_{bus}$ | Infinite bus voltage |
| $c_p$ | Aerodynamic power coefficient |
| $f$ | System frequency |
| $f^r$ | Rated frequency |
| $r_s$ | Resistance of a single phase of the stator windings |
| $r_l$ | Resistance of the grid connection impedance |
| $U_g^r$ | Rated collection grid voltage |
| $U_w^r$ | Rated wind turbine output voltage |
| $v_w$ | Wind speed |

**Greek symbols**

| | |
|---|---|
| $\Gamma_m$ | Generator torque |
| $\Gamma_t$ | Wind turbine torque |
| $\beta$ | Pitch angle |
| $\lambda_m$ | Flux linkage per rotating speed unit |
| $\nu$ | Gearbox multiplication ratio |
| $\omega_{mn}$ | Nominal generator speed |
| $\omega_r$ | Generator electrical angle speed |
| $\omega_t$ | Wind turbine speed |
| $\rho$ | Air density |
| $\tau$ | Time constant of the pitch angle controller |
| $\theta_m$ | Generator shaft angular position |
| $\theta_r$ | Generator rotor electric angle |

**Superscripts and Subscripts**

| | |
|---|---|
| $*$ | Reference value |
| $abc$ | Vector of *abc* components |
| $qd$ | Vector of *qd* components |
| $m$ | Variable related to the generator shaft |
| $r$ | Variable related to the generator rotor |
| $s$ | Variable related to the generator stator |
| $t$ | Variable related to the turbine |
| $z$ | Variable related to the grid connection point |

Zilong Gong, Junyu Mao, Adrià Junyent-Ferré and Giordano Scarciotti are with the Department of Electrical and Electronic Engineering, Imperial College London, London, SW7 2AZ, UK. {zilong.gong18, junyu.mao18, adria.junyent-ferre, g.scarciotti}@imperial.ac.uk.

## A. WIND FARM MODEL

In this section, we provide the full model of the wind turbine used in the simulations. The wind turbine model consists of several sub-blocks. We summarise each block in terms of inputs, outputs and detailed equations. The Park and inverse Park transformation of a rotation angle $\theta$ are indicated by $T(\theta)$ and $T^{-1}(\theta)$, respectively.

1) Wind turbine dynamics:
   Block inputs: $\theta_m^*$, $\Gamma_m$ and $v_w$.
   Block outputs: $\theta_m$ and $\omega_m$.

$$\beta(s) = \frac{1}{\tau s + 1}\theta_m^*(s),$$
$$c_p(\Lambda, \beta) = c_1(c_2\frac{1}{\Lambda} - c_3\beta - c_4\beta^{c_5} - c_6)e^{-c_7\frac{1}{\Lambda}},$$
$$\Gamma_t = \frac{1}{2}c_p\rho A v_w^3 \frac{1}{\omega_t}, \tag{1}$$
$$\omega_t = \frac{1}{I_t}(\Gamma_t + \nu\Gamma_m),$$
$$\dot{\theta}_m = \omega_m = \nu\omega_t,$$

where $[c_1 \cdots c_9]$ are wind turbine characteristic parameters and $\Lambda$ is defined as $\frac{1}{\Lambda} = \frac{1}{\lambda + c_8\beta} - \frac{c_9}{1 + \beta^3}$ with $\lambda = \frac{\omega_t R}{v_w}$.

2) Wind turbine speed controller:
   Block input: $\omega_m$.
   Block outputs: $\Gamma_m^*$ and $\theta_m^*$.

$$K_{C_p} = \frac{1}{2}\rho A R^3 \frac{c_1(c_2 + c_6 c_7)^3 e^{-\frac{c_2 + c_6 c_7}{c_2}}}{c_2^2 c_7^4}$$
$$\Gamma_m^* = K_{C_p}\omega_m^2, \tag{2}$$
$$\theta_m^*(s) = \frac{K_p s + K_i}{s}(\omega_m(s) - \omega_{mn}).$$

3) Generator dynamics:
   Block inputs: $v_s^{qd}$ and $\omega_m$.
   Block outputs: $i_s^{qd}$, $i_s^{abc}$ and $\Gamma_m$.

$$v_s^{qd} = \begin{bmatrix} r_s & \omega_r L_d \\ -\omega_r L_q & r_s \end{bmatrix} i_s^{qd} + \begin{bmatrix} L_d & 0 \\ 0 & L_q \end{bmatrix}\frac{d}{dt}i_s^{qd} + \lambda_m\omega_r\begin{bmatrix} 1 \\ 0 \end{bmatrix},$$
$$\Gamma_m = \frac{3}{2}P(\lambda_m i_{sq} + (L_d - L_q)i_{sq}i_{sd}),$$
$$i_s^{abc} = T^{-1}(\theta_r)i_s^{qd}, \tag{3}$$

4) Generator vector controller:
   Block inputs: $\Gamma_m^*$, $i_s^{abc}$, $\omega_m$ and $\theta_m$.
   Block outputs: $v_s^{qd}$ and $v_s^{abc}$.

$$i_s^{qd} = T(\theta_r)i_s^{qbc}$$

$$i_{sq}^* = \frac{2}{3P}\frac{\Gamma_m^*}{\lambda_m},$$

$$i_{sd}^* = \frac{2}{3P}\frac{Q_s^*}{\omega_m\lambda_m},$$

$$\hat{v}_{sq} = \frac{K_{pq}s + K_{iq}}{s}(i_{sq}^* - i_{sq}),$$

$$\hat{v}_{sd} = \frac{K_{pd}s + K_{id}}{s}(i_{sd}^* - i_{sd}),$$  (4)

$$v_s^{qd} = \hat{v}_s^{qd} + \begin{bmatrix} 0 & \omega_r L_d \\ -\omega_r L_q & 0 \end{bmatrix} i_s^{qd} + \lambda_m\omega_r \begin{bmatrix} 1 \\ 0 \end{bmatrix},$$

$$v_s^{abc} = T^{-1}(\theta_r)v_s^{qd}.$$

where $\omega_r = P\omega_m$, $\theta_r = P\theta_m$, $v_s^{qd} = [v_{sq}, v_{sd}]^{\text{T}}$, $\hat{v}_s^{qd} = [\hat{v}_{sq}, \hat{v}_{sd}]^{\text{T}}$ and $i_s^{qd} = [i_{sq}, i_{sd}]^{\text{T}}$.

5) DC bus dynamics:
  Block inputs: $i_l^{abc}$, $v_l^{abc}$, $i_s^{abc}$ and $v_s^{abc}$.
  Block outputs: $V_{DC}$ and $i_{DCm}$.

$$\frac{d}{dt}V_{DC} = \frac{1}{C}(i_{DCm} - i_{DCl}),$$

$$\{v_l^{abc}\}^{\text{T}}i_l^{abc} = V_{DC}i_{DCl},$$  (5)

$$\{v_s^{abc}\}^{\text{T}}i_s^{abc} = V_{DC}i_{DCm}.$$

6) Grid side system dynamics:
  Block inputs: $v_z^{abc}$ and $v_l^{abc}$.
  Block output: $i_l^{abc}$.

$$v_l^{abc} = r_l i_l^{abc} + L_l\frac{d}{dt}i_i^{abc} + v_z^{abc}.$$  (6)

7) Grid side controller:
  Block inputs: $V_{DC}$ and $i_{DCm}$.
  Block output: $i_{DCl}^*$.

$$i_{DCl}^* = \frac{K_{pg}s + K_{ig}}{s}(V_{DC}^* - V_{DC}) + i_{DCm}$$  (7)

8) Grid current controller
  Block inputs: $V_{DC}$, $i_{DCl}^*$, $v_z^{abc}$ and $i_l^{abc}$.
  Block output: $v_l^{abc}$.

$$i_{lq}^* = \frac{2}{3}\frac{V_{DC}}{v_{zq}}i_{DCl}^*,$$

$$i_{ld}^* = 0,$$

$$\hat{v}_{lq} = \frac{K_{pc}s + K_{ic}}{s}(i_{lq}^* - i_{lq}),$$

$$\hat{v}_{ld} = \frac{K_{pc}s + K_{ic}}{s}(i_{ld}^* - i_{ld}),$$

$$v_{lq} = v_{zq} - 2\pi f i_{ld}L_l - \hat{v}_{lq},$$  (8)

$$v_{ld} = 2\pi f i_{lq}L_l - \hat{v}_{ld},$$

$$\hat{\omega} = \frac{s + 0.129}{s}v_{zd},$$

$$i_l^{qd} = T(2\pi f t - \hat{\omega}t)i_l^{abc},$$

$$v_l^{qd} = T(2\pi f t - \hat{\omega}t)v_l^{abc}.$$

where $i_l^{qd} = [i_{lq}, i_{ld}]^{\text{T}}$, $v_l^{qd} = [v_{lq}, v_{ld}]^{\text{T}}$ and $v_z^{qd} = [v_{zq}, v_{zd}]^{\text{T}}$.

## B. WIND FARM PARAMETERS

In this section, we summarise the parameters of the wind farm used in the simulation.

1) Wind turbine: $c_1 = 1$, $c_2 = 39.52$, $c_6 = 2.04$, $c_7 = 14.47$, $c_3 = c_4 = c_5 = c_8 = c_9 = 0$, $R = 40$m, $A = 5,026.5\text{m}^2$, $\rho = 1.225\text{kg/m}^3$, $\nu = 90$, $I_t = 4\text{kg} \cdot \text{km}^2$, $\tau = 0.1$s and $v_w = 7\text{m/s}$.
2) Wind turbine speed controller: $\omega_{mn} = 1,602\text{min}^{-1}$, $K_p = 0.1° \cdot s/\text{rad}$ and $K_i = 0.02°/\text{rad}$.
3) Generator: 2 pairs of poles, $r_s = 15\text{m}\Omega$, $\lambda_m = 2.35\text{V·s/rad}$, $L_q = 0.12732\text{mH}$ and $L_d = 0.12764\text{mH}$.
4) Generator vector controller: $Q_s^* = 10\text{VAr}$, $K_{pq} = 0.0637\text{V/A}$, $K_{iq} = 7.5\text{V/(A} \cdot \text{s)}$, $K_{pd} = 0.0638\text{V/A}$ and $K_{id} = 7.5\text{V/(A} \cdot \text{s)}$.
5) DC bus: $C = 10\text{mF}$ and $V_{DC}^* = 2.6\text{kV}$.
6) Grid side system: $r_l = 20\text{m}\Omega$, $L_l = 1\text{mH}$, $U_w^r = 0.97\text{kV}$, $U_g^r = 66\text{kV}$ and $f^r = 50\text{Hz}$.
7) Grid side controller: $K_{pg} = 0.6032\text{A/V}$ and $K_{ig} = 14.2122\text{A/(V} \cdot \text{s)}$.
8) Grid current controller: $K_{pc} = 0.2803\text{V/A}$ and $K_{ic} = 10\text{V/(A} \cdot \text{s)}$.

## C. IEEE 14-BUS SYSTEM

In this section, we introduce the IEEE 14-bus model. This standard power system consists of 14 buses, 5 generators, 11 loads and 20 transmission lines. The diagram of the IEEE 14-bus model is presented in Fig. 1 [1].
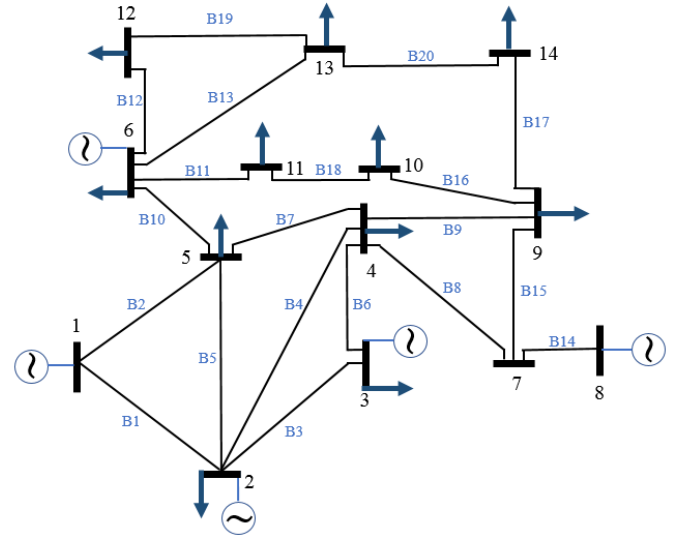


Fig. 1. The diagram of IEEE 14-bus system, indicating generators, loads positions and transmission lines.

## D. IEEE 14-BUS SYSTEM PARAMETERS

In this section, we summarise the bus parameters and line parameters of the modified IEEE 14-bus system in Table I and Table II, respectively.

TABLE I
BUS PARAMETERS OF 14-BUS SYSTEM

| Bus | Generation | | Load | |
|---|---|---|---|---|
| No. | Real(MW) | Reactive(MVAR) | Real(MW) | Reactive(MVAR) |
| 1 | 100.0 | -16.9 | 0.0 | 0.0 |
| 2 | 100.0 | 42.4 | 21.7 | 12.7 |
| 3 | 100.0 | 23.4 | 94.2 | 19.0 |
| 4 | 0.0 | 0.0 | 47.8 | 3.9 |
| 5 | 0.0 | 0.0 | 7.6 | 1.6 |
| 6 | 100.0 | 12.2 | 11.2 | 7.5 |
| 7 | 0.0 | 0.0 | 0.0 | 0.0 |
| 8 | 100.0 | 17.4 | 0.0 | 0.0 |
| 9 | 0.0 | 0.0 | 29.5 | 16.6 |
| 10 | 0.0 | 0.0 | 9.0 | 5.8 |
| 11 | 0.0 | 0.0 | 3.5 | 1.8 |
| 12 | 0.0 | 0.0 | 6.1 | 1.6 |
| 13 | 0.0 | 0.0 | 13.5 | 5.8 |
| 14 | 0.0 | 0.0 | 14.9 | 5.0 |

TABLE II
LINE PARAMETERS OF 14-BUS SYSTEM

| Bus | Between | Line impedance | | Half line |
|---|---|---|---|---|
| No. | buses | Resistance(pu) | Reactance(pu) | Susceptance(pu) |
| 1 | 1-2 | 0.01938 | 0.05917 | 0.02640 |
| 2 | 2-3 | 0.04699 | 0.19797 | 0.02190 |
| 3 | 2-4 | 0.05811 | 0.17632 | 0.01870 |
| 4 | 1-5 | 0.05403 | 0.22304 | 0.02460 |
| 5 | 2-5 | 0.05695 | 0.17388 | 0.01700 |
| 6 | 3-4 | 0.06701 | 0.17103 | 0.01730 |
| 7 | 4-5 | 0.01335 | 0.04211 | 0.0064 |
| 8 | 5-6 | 0.0 | 0.25202 | 0.0088 |
| 9 | 4-7 | 0.0 | 0.20912 | 0.0085 |
| 10 | 7-8 | 0.0 | 0.17615 | 0.0090 |
| 11 | 4-9 | 0.0 | 0.55618 | 0.0082 |
| 12 | 7-9 | 0.0 | 0.11001 | 0.0084 |
| 13 | 9-10 | 0.03181 | 0.08450 | 0.0079 |
| 14 | 6-11 | 0.09498 | 0.19890 | 0.0087 |
| 15 | 6-12 | 0.12291 | 0.25581 | 0.0092 |
| 16 | 6-13 | 0.06615 | 0.13027 | 0.0086 |
| 17 | 9-14 | 0.12711 | 0.27038 | 0.0089 |
| 18 | 10-11 | 0.8205 | 0.19207 | 0.0077 |
| 19 | 12-13 | 0.22092 | 0.19988 | 0.0098 |
| 20 | 13-14 | 0.17093 | 0.34802 | 0.0091 |

## E. ROBUST ANALYSIS OF ALGORITHM 1

To analyse the robustness of Algorithm 1, we add Gaussian noise to the measurements of $y(t)$ with signal-noise-ratio (SNR) of 60dB. We estimate the quantity $C\Pi$ by Algorithm 1 with 1000 and 30 measurements, respectively. Fig. 2 shows the regions between the upper and lower envelopes of all obtained magnitude plots of the ROMs obtained for the 20 realisations of the noise. In particular, the red regions refer to the estimation with 1000 measurements ($\widetilde{\nu} = 1000$), the blue regions refer to the estimation with 30 measurements ($\widetilde{\nu} = 30$) and the brown dashed lines represent the ideal estimation (no noise).
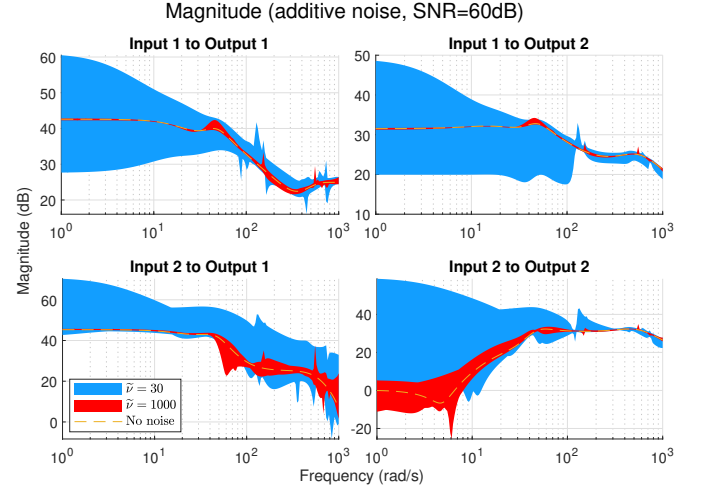


Fig. 2. Magnitude plots of the reduced-order models under 20 realizations of additive Gaussian noise. The red regions, blue regions and brown dashed lines refer to the estimation with 1000 measurements ($\widetilde{\nu} = 1000$), estimation with 30 measurements ($\widetilde{\nu} = 30$) and the ideal estimation (no noise), respectively.

## REFERENCES

[1] L. M. Leon, A. S. Bretas, and S. Rivera, "Quadratically constrained quadratic programming formulation of contingency constrained optimal power flow with photovoltaic generation," *Energies*, 2020.